# Optimized deep learning algorithms for application with data from PMD cameras

TECHNISCHE UNIVERSITÄT ILMENAU

H. Lietz*, M. Franzen*, J. Eberhardt* and S. Sinzinger**
* Faculty T - Technology and Management, University of Applied Sciences Ravensburg-Weingarten
** Department of Mechanical Engineering, Group of Optical Engineering, Ilmenau University of Technology

Hochschule Ravensburg-Weingarten University of Applied Sciences

## 1. Motivation: super-resolution (SR) on inherently related sensor data

Time-of-Flight (ToF) Photonic Mixing Device (PMD) camera
- fast and robust three-dimensional image acquisition
- PMD sensor measures the phase difference between an emitted and its reflected amplitude modulated IR signal in real time

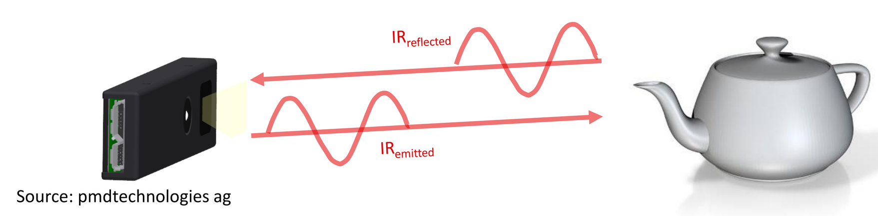

Source: pmdtechnologies ag

Problem
- large pixel sizes limit lateral resolution
- existing depth map SR fusion approaches require a further sensor's additional high-resolution (HR) intensity image

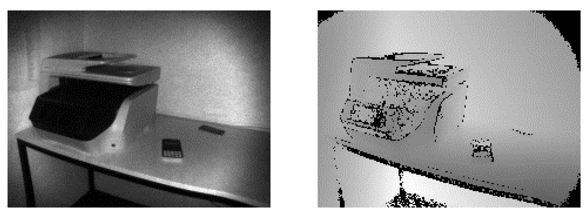
Amplitude and distance images from PMDtec's miniaturized PMD camera PicoFlexx.

Goal
SR strategy for self-sufficient resolution enhancement on ToF camera's output images
- amplitude image and
- depth map

using data accquired with only a single 3D PMD sensor.

## 2. State-of-the-art: dependence on additional HR intensity data

Single image super-resolution (SISR)
- currently, artificial intelligence learning-based algorithms reach the highest image quality in SISR results
- Convolutional Neural Networks (CNNs) learn either a per-pixel loss or a perceptual loss between its output and a ground truth image

Shallow → Deep

2014, SRCNN [1] [30.49 dB] → 2017, DRRN [2] [31.68 dB]

2014, SRCNN [1] [30.49 dB] → 2016, Perc. Loss [3] [27.09 dB]

2016, Perc. Loss [3] [27.09 dB] → 2017, **SRGAN**/SRResNet [4] [29.4 dB/ 32.05 dB] → 2017, **MDSR**/EDSR [5] [32.6 dB/ 32.62 dB]

2016, Perc. Loss [3] [27.09 dB] → 2017, **ENet** [6] [31.74 dB]

[dB]: ⌀ PSNR on *Set5* [7] @ 4x-scaling

Map on CNN based SISR methods (excerpt).

Guided depth map super-resolution (GDMSR)
- state-of-the-art methods for GDMSR are mostly optimization-based or learning-based algorithms
- GDMSR requires an additional high-resolution intensity image for guidance

Optimization-based: 2005, MRF [8] [RMSE = 2.24] → 2011, Park et al. [9] [RMSE = 1.82] → 2013, Ferstl et al. [10] [RMSE = 1.29] → 2017, Jung et al. [11] [RMSE = 1.26]

RMSE on Middlebury 2005 *Art disparity map* [12, 13] @ 4x-scaling

Learning-based: 2016, FCN-PDN [14] Deep CNN + variational optimization → 2016, Song et al. [15] Deep CNN + depth statistics and color-depth correlation → 2016, MSG-Net [16] Multi-Scale Guided CNN

Map on GDMSR methods (excerpt).

## 3. Contribution: independence from further sensor data

Step 1: Superresolve PMD sensor's low-resolution (LR) intensity image using *ENet-PAT* [6] CNN

**Perceptual loss**

$$\mathcal{L}_P = \|\Phi(I_{est}) - \Phi(I_{HR})\|_2^2$$
$$\Phi(I) = feature\ map\ of\ image\ I$$

→ Euclidean loss optimization on feature maps

**Adversarial training**

$$\mathcal{L}_A = -\log\left(D\left(G(z)\right)\right)$$
$$D = discriminative\ network$$
$$G(z) = generated\ sample$$

→ discriminative network trains mapping from LR images to HR images

**Texture matching loss**

$$\mathcal{L}_T = \left\|G\left(\Phi(I_{est})\right) - G\left(\Phi(I_{HR})\right)\right\|_2^2$$
$$G\left(\Phi(I)\right) = gram\ matrix\ of\ feature\ map\ \Phi(I)$$

→ enforces locally similar textures between SR result and HR ground truth

Step 2: Superresolve LR depth map using an *intensity guided SR* algorithm [11] with the SISR results from step 1

**Edge-aware weight**

$$W_{ID,p} = \begin{cases} f(W_I)\cdot\left(W_{D,p}+\varepsilon\right)^{\beta}, & \left(W_{I,p}-T_I\right)\cdot\left(W_{D,p}-T_D\right) < 0 \\ \left(W_{I,p}+\varepsilon\right)^{\alpha}\cdot\left(W_{D,p}+\varepsilon\right)^{\beta}, & otherwise \end{cases}$$

$W_{ID,p} = magnitude\ function$ $\quad W_D, W_I = magnitude\ of\ depth/intensity\ gradient$
$f(W_I) = constant\ for\ magnitude\ image\ W_I, balances\ W_{ID}\ for\ different\ cases\ of\ W_I$
$p = for\ a\ pixel$ $\quad \alpha,\beta,\varepsilon = positive\ constants$ $\quad T_I, T_D = pre-defined\ thresholds$

→ controls $L_0$ gradient regularization term to preserve edges and remove edge blurring and texture copying artifacts

**Weighted $L_0$ gradient minimization**

$$\min_{D_H}\left\{\sum_p \left(D_{H,p} - D_p\right)^2 + \frac{\lambda}{W_{ID,p}}\cdot H(\nabla D_{H,p})\right\}$$

$D_H = HR\ depth\ reconstruction$ $\quad D = HR\ depth\ estimation$
$\nabla D_{H,p} = gradient\ of\ D_H\ for\ a\ pixel\ p$ $\quad p = for\ a\ pixel$
$\lambda = positiv\ constant$ $\quad H\left(\nabla D_{H,p}\right) = binary\ function$

→ combines the original $L_0$ gradient minimization and the magnitude function $W_{ID,p}$

## 4. Results

4.1 SISR results on intensity images

Slanted edge | Art | PMDtec PicoFlexx

Ground truth

Bicubic Interpolation

ENet-PAT

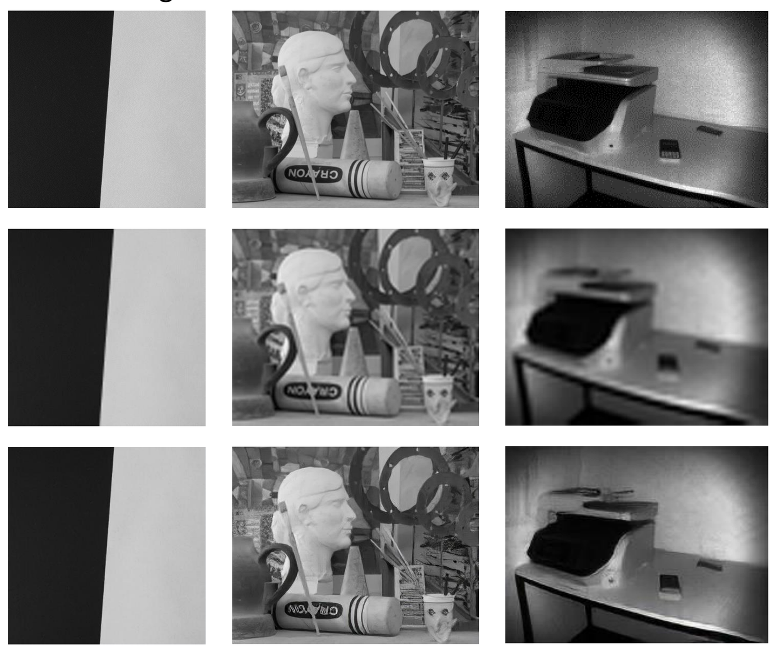

| SISR results on *Slanted edge* target | MTF50 [c/p] | PSNR [dB] | RMSE [a.u.] |
|---|---|---|---|
| Ground truth | 0.632 | Infinite | 0 |
| Bicubic interpolation | 0.105 | 34.37528 | 4.87277 |
| ENet-PAT SR result[1] | 0.497 | 41.46295 | 2.15473 |

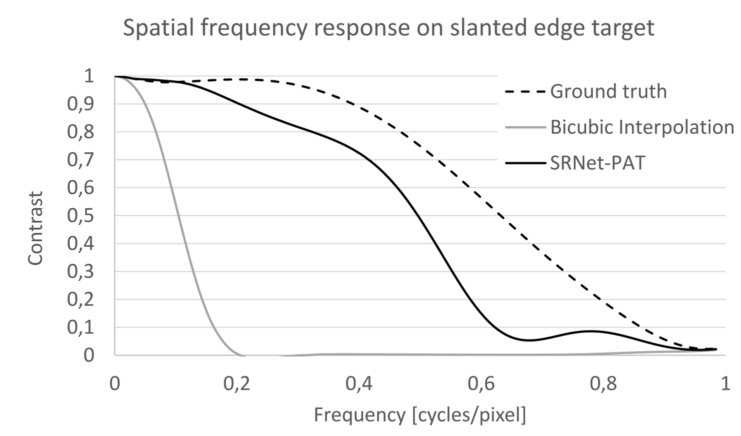

Spatial frequency response is measured with MTFMapper [17].

| Intensity image [PSNR in dB / RMSE a.u.] | Synthetic: Middlebury 2005 dataset [12, 13] *Art* | Books | Moebius | Real data: *PMDtec PicoFlexx* |
|---|---|---|---|---|
| Nearest neighbor interp. | 23.78783 / 16.48726 | 24.05217 / 15.99306 | 26.39474 / 12.21247 | 25.50144 / 13.53532 |
| Bicubic interpolation | 25.32300 / 13.81626 | 25.48541 / 13.56031 | 27.82000 / 10.36430 | 26.90039 / 11.52181 |
| ENet-PAT SR result[1] | 26.63320 / 11.88174 | 26.57402 / 11.96297 | 28.10751 / 10.02685 | 29.52067 / 8.52131 |

[1]Pre-trained reference implementation of ENet-PAT [6] for magnification ratio of 4

4.2 GDMSR results on depth maps

Ground truth depth | Ground truth guided | Bicubic guided | ENet-PAT guided

Art (noise-free)

Art (noisy[2])

Real data: PMDtec PicoFlexx

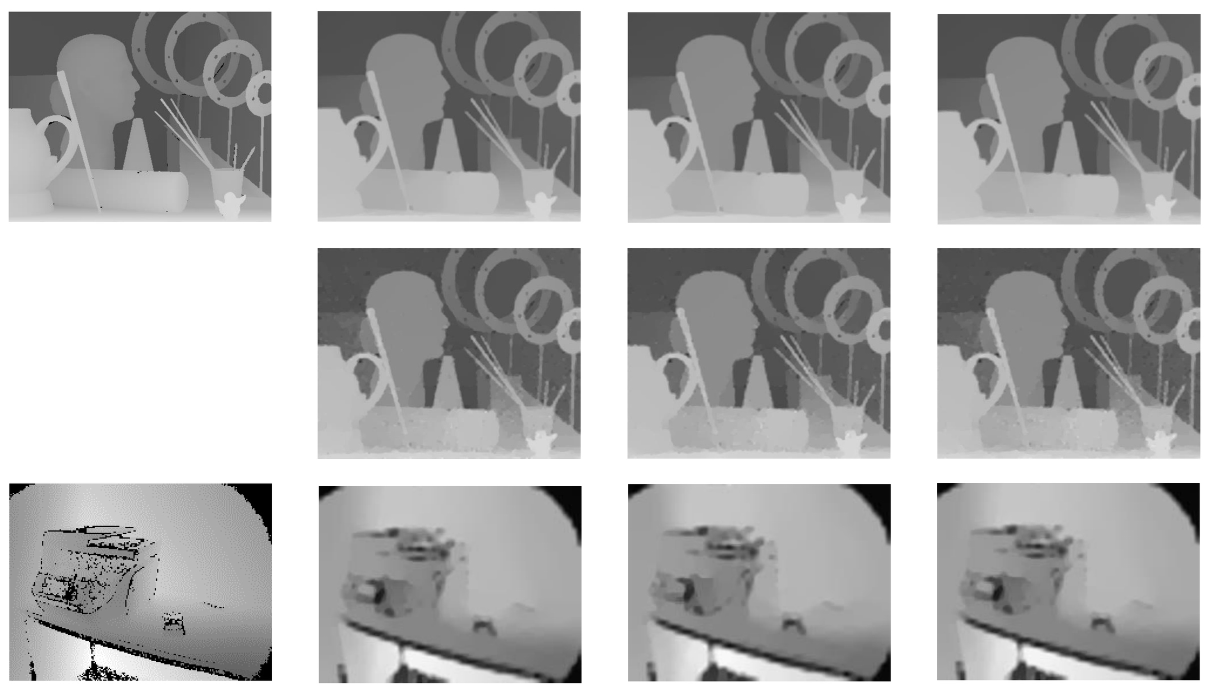

| Depth image [PSNR in dB / RMSE a.u.] | | Synthetic: Middlebury 2005 dataset [12, 13] *Art* | Books | Moebius | Real data: *PMDtec PicoFlexx* |
|---|---|---|---|---|---|
| Noise-free LR depth maps | Ground truth guided | 29.12408 / 8.91941 | 28.93634 / 9.11429 | 30.11049 / 7.96188 | |
| | Nearest neighbor guided | 27.85658 / 10.32075 | 28.49669 / 9.58751 | 29.37705 / 8.66339 | |
| | Bicubic guided | 28.99904 / 9.04874 | 28.75584 / 9.30568 | 29.76623 / 8.28378 | |
| | ENet-PAT guided | **29.11472 / 8.92903** | **28.97976 / 9.06884** | **30.04139 / 8.02547** | |
| Noisy[2] LR depth maps | Ground truth guided | 28.92745 / 9.12363 | 28.90592 / 9.14627 | 30.00915 / 8.05532 | 18.17230 / 31.47205 |
| | Nearest neighbor guided | 27.88768 / 10.28387 | 28.56610 / 9.51120 | 29.39432 / 8.64617 | 17.85728 / 32.63442 |
| | Bicubic guided | 28.78891 / 9.27032 | 28.74017 / 9.32249 | 29.82468 / 8.22822 | 18.10915 / 31.70173 |
| | ENet-PAT guided | **28.78996 / 9.26920** | **28.95732 / 9.09230** | **29.91369 / 8.14434** | **18.16454 / 31.50019** |

[2]Synthetic images are imposed by additive white Gaussian noise with variance $\sigma^2 = 0.001$

## 5. Conclusions & Outlook

SISR
- good performance on simple *slanted edge* target
  → SR result reaches nearly 78 % of ground truth's MTF50-value
  → ENet-PAT's PSNR value is around 1.2 times higher than bicubic interpolation ones
- less image quality on *Art* and *PMDtec PicoFlexx* images
  → fine details are missing
  → ENet-PAT's PSNR is only 1.05 times and 1.1 times higher than bicubic interpolation ones for *Art* and *PMDtec PicoFlexx*, respectivley

GDMSR
- image quality is nearly the same for ground truth guided and SISR guided SR depth map results
- moderate overall performance
  → even the ground truth guided SR results on noise-free LR inputs look blurry
  → image quality is worse for real data and noisy synthetic images

Outlook
- increase image quality of SISR results by using own training data
- enhance real depth map's image quality by inpainting invalid pixel regions before applying the SR method
- investigate further (learning-based) GDMSR algorithms

**References**

[1] C. Dong, C. C. Loy, K. He, and X. Tang, "Image Super-Resolution Using Deep Convolutional Networks", in IEEE Transactions on Pattern Analysis and Machine Intelligence 38 (2), (2014)
[2] Y. Tai, J. Yang, and X. Liu, "Image Super-Resolution via Deep Recursive Residual Network", in IEEE Conference on Computer Vision and Pattern Recognition (CVPR), (2017)
[3] J. Johnson, A. Alahi, and L. Fei-Fei, "Perceptual Losses for Real-Time Style Transfer and Super-Resolution", in 14th European Conference on Computer Vision (ECCV), (2016)
[4] C. Ledig, L. Theis, F. Huszár, J. Caballero, A. Cunnignham, A. Acosta, A. Aitken, A. Tejani, J. Totz, Z. Wang, and W. Shi, "Photo-Realistic Single Image Super-Resolution Using a Generative Adversarial Network", in IEEE Conference on Computer Vision and Pattern Recognition (CVPR), (2017)
[5] B. Lim, S. Son, H. Kim, S. Nah, and K. Mu Lee, "Enhanced Deep Residual Networks for Single Image Super-Resolution", in IEEE Conference on Computer Vision and Pattern Recognition Workshops (CVPRW), (2017)
[6] M.S.M. Sajjadi, B. Schölkopf, and M. Hirsch, „EnhanceNet: Single Image Super-Resolution through Automated Texture Synthesis" in International Conference on Computer Vision, (2017)
[7] M. Bevilacqua, A. Roumy, C. Guillemot, and M.L. Alberi-Morel, "Low-Complexity Single-Image Super-Resolution based on Nonnegative Neighbor Embedding", in British Machine Vision Conference (BMVC), (2012)
[8] J. Diebel, and S. Thrun, "An Application of Markov Random Fields to Range Sensing", in Proceedings of Conference on Neural Information Processing Systems (NIPS), (2005)
[9] J. Park, H. Kim, Y.W. Tai, M.S. Brown, and I. Kweon, "High Quality Depth Map Upsampling for 3D-TOF Cameras", in International Conference on Computer Vision (ICCV), (2011)
[10] D. Ferstl, C. Reinbacher, R. Ranftl, M. Rüther, and H. Bischof, "Image Guided Depth Upsampling using Anisotropic Total Generalized Variation", in IEEE International Conference on Computer Vision (ICCV), (2013)
[11] C. Jung, S. Yu, and J. Kim, "Intensity-guided edge-preserving depth upsampling through weighted $L_0$ gradient minimization", in J. Vis. Commun. Image R. 42, (2017)
[12] H. Hirschmüller, and D. Scharstein, "Evaluation of Cost Functions for Stereo Matching", in IEEE Conference on Computer Vision and Pattern Recognition (CVPR), (2007)
[13] D. Scharstein, and C. Pal, "Learning Conditional Random Fields for Stereo", in IEEE Conference on Computer Vision and Pattern Recognition (CVPR), (2007)
[14] G. Riegler, D. Ferstl, M. Rüther, and H. Bischof, "A Deep Primal-Dual Network for Guided Depth Super-Resolution", in Proceedings of the British Machine Vision Conference (BMVC), (2016)
[15] X. Song, Y. Dai, and X. Qin, "Deep Depth Super-Resolution: Learning Depth Super-Resolution Using Deep Convolutional Neural Network", in 13th Asian Conference on Computer Vision (ACCV), (2016)
[16] T.W. Hui, C.C. Loy, and X. Tang, "Depth Map Super-Resolution by Deep Multi-Scale Guidance", in 14th European Conference on Computer Vision (ECCV), (2016)
[17] F. van den Bergh, "Deferred slanted-edge analysis: a unified approach to spatial frequency response measurement on distorted images and color filter array subsets", in Journal of the Optical Society of America A 35 (3), (2018)

University of Applied Sciences Ravensburg-Weingarten
Faculty T – Technology and Management
Doggenriedstraße
88250 Weingarten, Germany

Laboratory for 3D Camera Technology and Technical Optics
Henrik Lietz, +49 (0) 751/501-9283
henrik.lietz@hs-weingarten.de

DGaO-Proceedings 2018 - http://www.dgao-proceedings.de - ISSN: 1614-8436 - urn:nbn:de:0287-2018-P028-5
eingegangen: 22.05.2018 veröffentlicht: 25.06.2018